Biochimica et Biophysica Acta 1863 (2016) 91–101

Contents lists available at ScienceDirect

Biochimica et Biophysica Acta

journal homepage: www.elsevier.com/locate/bbamcr

Evolution and structural organization of the mitochondrial contact site (MICOS) complex and the mitochondrial intermembrane space bridging (MIB) complex

Martijn A. Huynen [a,b,*], Mareike Mühlmeister [b], Katherina Gotthardt [b,c], Sergio Guerrero-Castillo [b,c], Ulrich Brandt [b,c]

[a] Centre for Molecular and Biomolecular Informatics, Radboud Institute for Molecular Life Sciences, Radboud University Medical Center, Nijmegen, The Netherlands
[b] Nijmegen Centre for Mitochondrial Disorders, Radboud University Medical Center, Nijmegen, The Netherlands
[c] Cluster of Excellence Frankfurt "Macromolecular Complexes", Goethe-University, Germany

ARTICLE INFO

Article history:
Received 27 July 2015
Received in revised form 25 September 2015
Accepted 14 October 2015
Available online 23 October 2015

Keywords:
MICOS
MIB
C19orf70
HemX
Complexome profiling
Metaxin 3

ABSTRACT

We have analyzed the distribution of mitochondrial contact site and cristae organizing system (MICOS) complex proteins and mitochondrial intermembrane space bridging complex (MIB) proteins over (sub)complexes and over species. The MICOS proteins are associated with the formation and maintenance of mitochondrial cristae. Indeed, the presence of MICOS genes in genomes correlates well with the presence of cristae: all cristae containing species have at least one MICOS gene and cristae-less species have none. Mic10 is the most widespread MICOS gene, while Mic60 appears be the oldest one, as it originates in the ancestors of mitochondria, the proteobacteria. In proteobacteria the gene occurs in clusters with genes involved in heme synthesis while the protein has been observed in intracellular membranes of the alphaproteobacterium *Rhodobacter sphaeroides*. In contrast, Mic23 and Mic27 appear to be the youngest MICOS proteins, as they only occur in opisthokonts. The remaining MICOS proteins, Mic10, Mic19, Mic25 and Mic12, the latter we show to be orthologous to human C19orf70/QIL1, trace back to the root of the eukaryotes. Of the remaining MIB proteins, also DNAJC11 shows a high correlation with the presence of cristae. In mitochondrial protein complexome profiles, the MIB complex occurs as a defined complex and as separate subcomplexes, potentially reflecting various assembly stages. We find three main forms of the complex: A) The MICOS complex, containing all the MICOS proteins, B) a membrane bridging subcomplex, containing in addition SAMM50, MTX2 and the previously uncharacterized MTX3, and C) the complete MIB complex containing in addition DNAJC11 and MTX1.

1. Introduction

Cristae are highly variable invaginations of the inner mitochondrial membrane that are needed for providing a sufficient area and the proper spatial organization for the multiprotein complexes of oxidative phosphorylation and other membrane integral proteins required for mitochondrial function. Since their discovery in rat cells by George Palade [1,2], they have been observed in many eukaryotes, including, already in 1955, ciliates and amoebozoa [3], in 1958 in plants [4] and more recently even in species with atypical, hydrogen producing mitochondria [5]. Since 2005 the critical involvement of the mitochondrial contact site (MICOS) proteins with cristae (reviewed in [6], and given a uniform nomenclature in [7]), has been described, but only in a limited number of animal and fungal species including human [8], *Saccharomyces cerevisiae* [9], *Caenorhabditis elegans* [10] and recently *Drosophila melanogaster* [11]. MICOS interacts with components of the sorting and assembly machinery (SAM) complex [12] of the outer membrane [13] to form the mitochondrial intermembrane space bridging (MIB) complex [14].

Here we set out to map the evolution of the MIB complex using the presence of its genes among sequenced genomes and the presence of its proteins among mitochondrial proteomes, and compare that with the documented presence and absence of mitochondrial cristae. Such detailed evolutionary analyses of mitochondrial systems have predicted proteins involved in a complex based on newly detected homology of human proteins to yeast proteins [15] and have predicted new candidate proteins for a molecular system via their co-evolution with proteins already known to be part of that system [16,17]. Furthermore, they facilitate studies in model species, specifically when the detection of orthologs is not trivial due to high rates of sequence evolution or gene duplications. Finally, they allow us to trace evolution along an evolutionary tree and correlate the gain and loss of genes with phenotypic characteristics of the species.

* Corresponding author at: Centre for Molecular and Biomolecular Informatics, Radboud University Medical Center PO Box 9101, 6500 HB Nijmegen, The Netherlands.
E-mail address: huynen@cmbi.ru.nl (M.A. Huynen).

http://dx.doi.org/10.1016/j.bbamcr.2015.10.009

Evolution of the MICOS proteins of the MIB complex has been addressed with respect to homology relationships between human and *S. cerevisiae* [6,7], while the evolution across the eukaryotes of some of the outer mitochondrial membrane proteins of MIB has been addressed in specific reviews [18,19]. Furthermore, while this manuscript was nearing completion, MICOS evolution has also been assessed across the eukaryotes [20]. Given the volatility of orthology prediction in the "twilight zone," where even homology relationships are not obvious due to low levels of sequence identity, we have mapped the distribution of the MIB genes among the eukaryotes with and without cristae independently of that study. Furthermore, we examined in proteomics data sets whether predicted MIB proteins have been observed in mitochondrial fractions, or, in (alpha)proteobacteria, in their membrane fractions.

To corroborate and complement the predictions from our evolutionary analysis, we further studied the composition of the MIB complex and its subcomplexes in detail by complexome profiling [21] revealing its modular design and defining MTX3 (metaxin 3) as a previously unidentified component of the complex.

2. Methods

2.1. Sequence analysis

For homology detection we used profile-based sequence analysis tools: JACKHMMER [22], HHpred [23] and the database PFAM [24]. For orthology prediction, when low sequence similarity precludes the generation of reliable phylogenies, we employed reciprocal best hit searches at the sequence profile level to obtain best-bidirectional hits: i.e. we ask whether a sequence-profile based on e.g. a protein family in the fungi has a reciprocal best hit with a sequence profile based on a protein family in plants. This technique has been successful in detecting orthology between rapidly evolving proteins with the same function in human and yeast mitochondria that had gone unnoticed in pairwise sequence comparisons, or in comparisons of sequences against a Hidden Markov Model [15]. We examined existing phylogenies from Treefam [25] to determine when gene duplications of MIB genes occurred in the evolution of the human lineage. The proteins predicted to be orthologous to human MICOS and MIB proteins, including the various aliases of the human proteins are in the supplementary material (Table S1).

2.2. Mitochondrial proteomics data

We examined mitochondrial proteomics datasets for the presence of MICOS orthologs from the following (model) species: *Arabidopsis thaliana*, *Chlamydomonas rheinhardtii*, *Schizosaccharomyces pombe*, *Neurospora crassa*, *Homo sapiens*, *Mus musculus*, *Tetrahymena thermophila*, *Caenorhabditis elegans*, *Drosophila melanogaster*, *Dictyostelium dicoideum* and *Rhodobacter sphaeroides*. For this we used the tables with the publications, dedicated databases like MitoMiner [26] and Pubmed Central.

2.3. Cell culture and isolation of mitochondria

Human osteosarcoma 143B cells were grown in tissue-culture flasks in DMEM (LONZA BE12-733F) supplemented with 10% fetal calf serum, 2 mM L-glutamine (Sigma G7513), 1 mM sodium pyruvate (Sigma S8636) and Minimum Essential Medium (MEM) non-essential amino acids (Sigma M7145) at 37 °C/5% CO_2. 143B cells were passaged 2–3 times a week using a trypsin/EDTA solution (Sigma, T4174) for detachment of the cells. Mitochondria were isolated from 143B cells by differential centrifugation at 4 °C as previously described [21]. At ~90% confluence, cells were washed twice with phosphate buffered saline, harvested after trypsination and sedimented by centrifugation at 1000 × g for 10 min. Cells were washed with ice-cold 0.9% NaCl and subsequently with 250 mM sucrose, 1 mM EDTA, 20 mM Tris/HCl pH 7.4. After resuspending in the same buffer supplemented with protease inhibitor (SigmaFAST S8830) cells were disrupted by 12 strokes through a 21G cannula attached to a 20 ml syringe. Nuclei, cell debris and intact cells were then removed by a low-speed centrifugation step (1000 × g, 10 min). After transfer of the supernatant into a new tube, mitochondria were pelleted by centrifugation at 6000 × g for 10 min. Mitochondria were resuspended in 250 mM sucrose, 1 mM EDTA and 2 mM Tris/HCl pH 7.4. Protein concentration was determined using the Lowry method.

Human skin fibroblasts were cultured in M199 medium (Gibco, 31,150) supplemented with 10% fetal calf serum and 100 U/ml penicillin/100 μg/ml streptomycin (Sigma, P4333) at 37 °C/5% CO_2. Cells were passaged once a week using a trypsin/EDTA solution (Sigma, T4174) for detachment of the cells. To prepare mitochondria, frozen fibroblast cell pellets were resuspended in ice-cold 10 mM Tris–HCl, pH 7.6 and incubated for 5 min on ice. The cells were homogenized using a glass/Teflon homogenizer at 0 °C. The homogenate was mixed with 1.5 M sucrose at a ratio of 1:0.25 and subsequently centrifuged at 600 × g at 2 °C for 10 min to remove nuclei, cell debris and intact cells. This centrifugation step was repeated with the supernatant to further purify the mitochondria, which were afterwards pelleted by a high-speed centrifugation at 14.000 x g at 2 °C for 10 min. The mitochondrial pellet was resuspended in phosphate buffered saline.

2.4. Complexome profiling

Mitochondria were solubilized at 10 mg/ml with 9 mg digitonin/mg protein in 50 mM NaCl, 5 mM 6-aminohexanoic acid, 1 mM EDTA, 50 mM imidazole/HCl pH 7.0. After centrifugation at 22,000 × g for 20 min the supernatant was applied to a 4–12% gradient blue-native electrophoresis (BNE) gel [27] using 50–150 μg protein per lane. Electrophoresis was performed in the cold room.

After BNE, each gel lane was prepared for complexome profiling as described previously [21]. The BNE gel was stained in colloidal Coomassie solution (0.02% Coomassie brilliant blue-G250, 5% aluminiumsulfate-(14–18)-hydrate, 10% ethanol, 2% ortho-phosphoric acid) overnight. After destaining with colloidal destainer (10% ethanol, 2% ortho-phosphoric acid) the gel was washed twice in ultrapure water for 30 min. Next the destained gel lanes were cut into 60 even slices that were then cut into small pieces, which were transferred into a well of a 96-well filter plate (Millipore, MABVN1250). The in-gel tryptic digest was essentially performed as described previously [28]. The gel pieces were incubated for 60 min in buffer containing 5 mM dithiothreitol, 50 mM ammonium hydrogen carbonate (AHC) followed by incubation in 15 mM 2-chloroacetamide, 50 mM AHC for 45 min. Gel slices were then washed with 50% methanol, 50 mM AHC for 15 min and air-dried for 45 min. The dehydrated gel pieces were swollen in 20 μl 5 ng/μl trypsin (Promega, V5111), 50 mM AHC, 1 mM $CaCl_2$ for 30 min at 4 °C. After addition of 50 μl 50 mM AHC, the plates were sealed and incubated over night at 37 °C for tryptic digest. The peptides were eluted by centrifugation into a 96-well PCR microplate and the remaining peptides were extracted twice in 50 μl 30% acetonitrile, 3% formic acid. The supernatants were dried in a SpeedVac concentrator and the peptides resuspended in 20 μl 5% acetonitrile, 0.5% formic acid.

The tryptic peptides were analyzed by liquid chromatography tandem mass spectrometry (LC-MS/MS) in a Thermo Scientific Q Exactive 2.0 Orbitrap Mass Spectrometry System equipped with a nano-flow high performance liquid chromatography system Easy nLC-1000 at the front end and the Thermo Scientific Xcalibur 2.2 SP1 Software Package [29]. Peptides were separated on 3 μm reprosil-pur C18 beads (Dr Maisch GmbH, Germany) filled into a PicoTip emitter column (8 ± 1 μm Silica Tip; New Objectives, USA) in 40 min HPLC runs using a 30 min gradient of 5% to 35% acetonitrile with 0.1% formic acid, followed by a column wash with 80% acetonitrile and re-equilibration with 5% acetonitrile for 5 min each. Peptides were analyzed on-line in positive mode by a mass spectrometry method programmed to fragment the top 20 most abundant peptides. Full scan MS mode (400 to 1400 m/z)

was operated at a resolution of 70 000 with automatic gain control (AGC) target of 1×10^6 ions and a maximum ion transfer of 20 ms. Selected ions for MS/MS were analyzed using the following parameters: resolution 17,500; AGC target of 1×10^5; maximum ion transfer of 50 ms; 4.0 m/z isolation window; for CID a normalized collision energy 30% was used; and dynamic exclusion of 30.0 s. A lock mass ion (m/z = 445.12) was used for internal calibration [30].

2.5. Protein identification

The analysis of the RAW files was performed using the MaxQuant software package (version 1.4.1.2 and 1.5.0.25, www.maxquant.org [31]). The extracted spectra were matched against the reviewed *H. sapiens* NCBI RefSeq database release 55. Sequences of known contaminants were added to this database and the reverse decoy was strictly set to FDR of 0.01. Database searches were done with 20 ppm and 0.5 Da mass tolerances for precursor ions and fragmented ions, respectively. Trypsin (two missed cleavages allowed) was selected as the protease. Dynamic modifications included N-terminal acetylation and oxidation of methionine. Cystein carbamidomethylation was set as a fixed modification. Keratins, hemoglobins and trypsin were removed from the list.

2.6. Data analysis

Protein abundancies were determined by label-free quantitation using the composite IBAQ intensity values determined by MaxQuant [31] and normalized within single or multiple migration profiles of individual proteins. The profiles were hierarchically clustered by distance measures based on Pearson correlation coefficient (uncentered) and the average linkage method and further analyzed by manual correlation profiling. The clustering and the visualization and analysis of the heat maps were done with the NOVA software v0.5 [32]. Exported data were further processed in Microsoft Excel. The mass calibration for the 4–12% BNE gels was performed using respiratory chain complexes and supercomplexes as standards as previously described [21].

3. Results

We started by a detailed mapping of the MIB proteins across cellular species. There are many names for the MICOS proteins, but in the main text we will use the MIC# names recently introduced by the field [7]. With respect to the outer membrane proteins of MIB we included SAMM50, MTX1, MTX2 (metaxin 1, 2) and DNAJC11 that have been observed to interact with the MICOS complex, and MTX3 (metaxin 3) that we observed to be part of the MIB complex (see below). The species in which we have mapped the presence of MIB proteins are the species with experimental data about MIB proteins: *S. cerevisiae*, *C. elegans* [10], *D. melanogaster* [11], *H. sapiens*, *Trypanosoma brucei* [33], *Entamoeba histolytica* [34], the species in which cristae have been reported to be present or appear to be absent in EM pictures (*Encephalotozoon cuniculi* [35], *Entamoeba histolytica* [36], *Giardia intestinalis* [37], *Trichomonas vaginalis* [38]) and for which genomes are available, species with mitochondrial proteomics data, species that cover the main branches of the eukaryotic tree of life, and finally alphaproteobacteria, the ancestors of the mitochondrial membranes. Apart from the presence of an ortholog, we also recorded whether a genome contains multiple orthologs (Fig. 1) as the result of a recent gene duplication.

3.1. Mic10

Mic10 (MINOS1/DUF543/UPF0327) is generally well conserved among eukaryotes and has a wide phylogenetic distribution (Fig. 1), indicating that it was invented at the root of the eukaryotes. Mic10 in fungi and in metazoa have been noted to have conserved glycine rich motifs in their two transmembrane helices [39], that have been shown to be required for oligomerization of the protein which, in turn, is required for obtaining membrane curvature [40,41]. Indeed these glycine-rich motifs (at least GxxxG, and often GxGxGxG) can be observed in Mic10 throughout the eukaryotes and are specifically well conserved in the second transmembrane helix (Figure S1). Notably in species distantly related to human some of the glycine residues are replaced by the other small amino acids alanine and serine, consistent with the role of these amino acids in packing transmembrane helices [42]. The *A. thaliana* [43] and *S. pombe* [44] Mic10 orthologs have been observed among mitochondrial proteins. Mic10 is however not universal among eukaryotes and appears to have been lost independently multiple times in species without an electron transfer chain and without cristae, and in the minimal oxidative phosphorylation system (complexes III, IV and V) containing *Plasmodium* species. It can however be found in a species with a alternative minimal oxidative phosphorylation system: a homolog is present in *Blastocystis sp.*, a species that does have cristae [45] and has complexes I and II but not complexes III, IV and V [46]. *Cryptosporidium parvum* has no mitochondrial genome, but its mitosomes have highly folded "cristae-like" inner membranes [47]. It is the only known species having cristae-like structures and a MICOS protein but lacking mitochondrially encoded oxidative phosphorylation complexes. These observations are consistent with the earlier report on the phylogenetic distribution of Mic10 [20].

3.2. Mic12

Mic12 (Aim5) is a short, rapidly evolving protein and simple, pairwise sequence homology detection did not allow detection of orthologs outside of the fungi [6]. Indeed, pairwise sequence comparisons with Blast do not even detect homologs outside the *Saccharomycetales* branch of the fungi. In addition, the recent analysis that compared sequence-profiles against individual sequences [20] did not detect homologs outside the fungi. To improve homology detection we here used sequence-profile to sequence-profile searches: exploiting sequence conservation among separate families of proteins to determine potential homology between them. We created a sequence profile with the yeast protein, using JACKHMMer [22] and used the profile-profile comparison tool HHpred [23] to compare it against existing sequence profiles of human proteins. The candidate human homolog of Mic12, C19orf70/LOC125988/QIL1 (E = 0.00045) is localized mainly in mitochondria [48], and was once observed to be part of the mitochondrial proteome [49]. A reciprocal search, based on an alignment of C19orf70 homologs among metazoa recovered the yeast protein as best hit, albeit, at a barely significant E-value (E = 0.043). Finally, we created a combined alignment of all metazoan and fungal homologs, and used that to search against the *A. thaliana* sequence profiles with HHpred. The putative ortholog AT2g28430 (E = 0.037) has once been found in mitochondrial fractions to co-migrate with complex I [50], a finding that however could not be reproduced in a more dedicated complex I study [51]. Based on the human, yeast and *A. thaliana* proteins and their detectable homologs we obtained an alignment of the Mic12 family (Fig. 2), where it should be noted that creating an alignment in itself cannot be considered as proof that these proteins are indeed homologous. As might have been expected based on the high E-values, the Mic12 family has very little sequence conservation beyond a hydrophobic amino-terminus, corresponding to a likely transmembrane region, and a "WN" motif that is preceded by a charged amino acids (Fig. 2). The periodicity of 3–4 amino acids in conservation of a hydrophobic amino acid (Fig. 2) suggests the presence of an amphipathic helix. QIL1/C19orf70 was recently identified to indeed interact with the MICOS complex in cultured human cells [11], which was confirmed by our complexome profiling analysis of the MICOS complex reported below. This corroborates our prediction that QIL1/C19orf70 is indeed the ortholog of Mic12 from yeast. Nevertheless, very little is known about the role of Mic12 in *S. cerevisiae* and further experimental analyses will be required to confirm that it has the same role in the MICOS complex as QIL1/C19orf70 in *H. sapiens*.

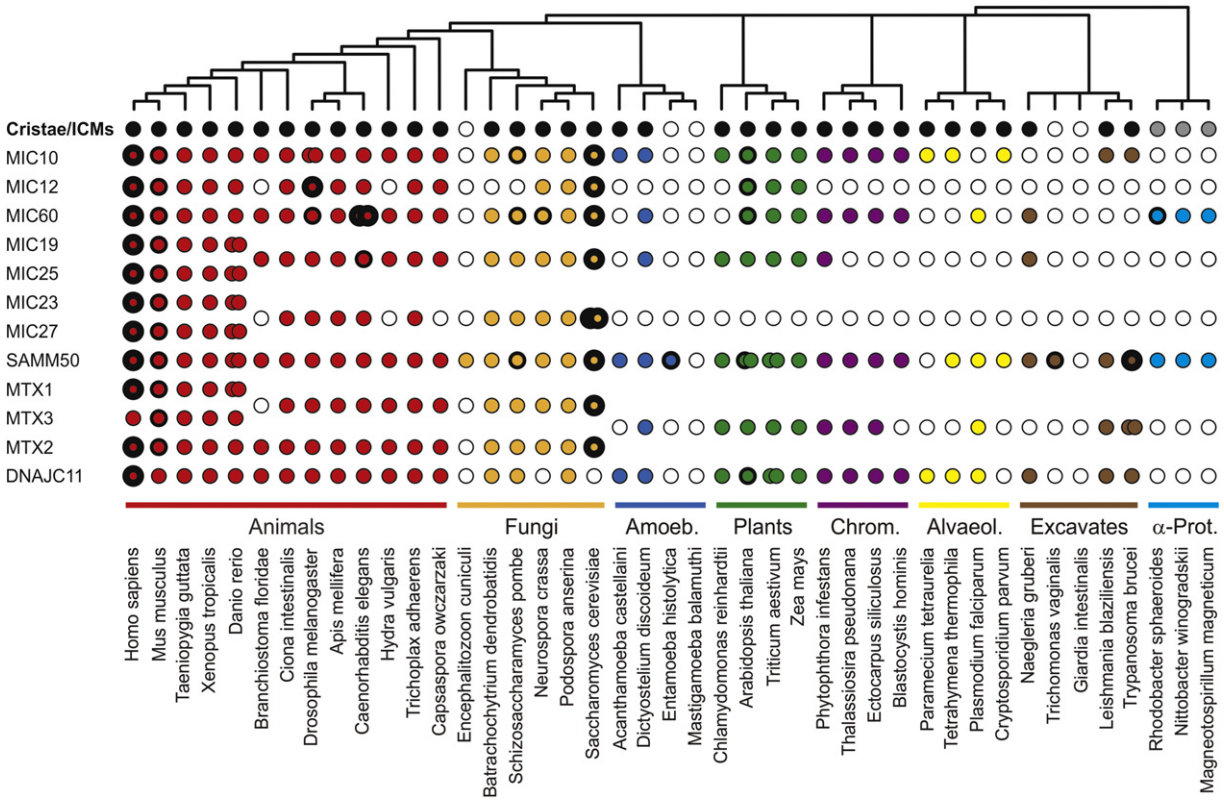

Fig. 1. *Phylogenetic distribution of MICOS and MIB subunits* The phylogenetic distribution of MICOS and MIB subunits was determined among eukaryotes with and without cristae (black), and among alphaproteobacteria with intracellular cytoplasmic membranes (ICM, gray). Levels of experimental evidence for a role in mitochondria or cristae formation are indicated: empty circles denote the absence of an ortholog from the sequenced genome, colored circles with a thin rim, the presence of an orthologous gene, medium rims denote the presence of the protein in a mitochondrial or ICM fraction. A thick rim indicates experimental evidence that the protein functions in mitochondria, e.g. via the presence of a phenotype, or a measured interaction with other proteins of the MIB complex. Double circles indicate the presence of two or more genes that are the result of a taxon-specific duplication. The results with respect to the presence/absence of an ortholog of the MICOS proteins are consistent with [20], except for the presence of Mic12 in metazoa and plants, and the presence of Mic19/25 orthologs outside the opisthokonts. Amoeb. = Amoebozoa, Alveol. = Alveolata, Chrom. = chromists, α-prot = Alphaproteobacteria.

3.3. Mic19 and Mic25

Human and yeast MIC19 (CHCHD3/MINOS3/CHCH-3/Aim13) and human MIC25 (CHCHD6/CHCM1) are part of the CHCH protein family (also called twin Cx9C family) that also contains other IMS proteins like COX23, COX19 and Mia40 [52]. As these proteins are part of a gene family, one requires phylogenetic approaches to separate the various orthologous groups from each other. Within the metazoa the Mic19/25 phylogeny indicates that human MIC19 and MIC25 result from a gene duplication at the root of the vertebrates [25] which is consistent with their phylogenetic distribution (Fig. 1). They are thus both orthologous to Mic19 in yeast and likely the result of the whole genome duplication at the root of the vertebrates, a pattern that has been observed often for mitochondrial proteins [53]. The short length and rapid evolution of this family however preclude the use of rigorous phylogenetic approaches to determine orthologous relationships in more distantly related species like plants [20]. We have therefore used the reciprocal-best-hit approach at the levels of sequence profiles [15] to determine orthologous relations, allowing us to extend orthology relations beyond the fungi and the metazoa, to amoebozoa (*Dictoystelium*), chromists (*Phytoptora*) and

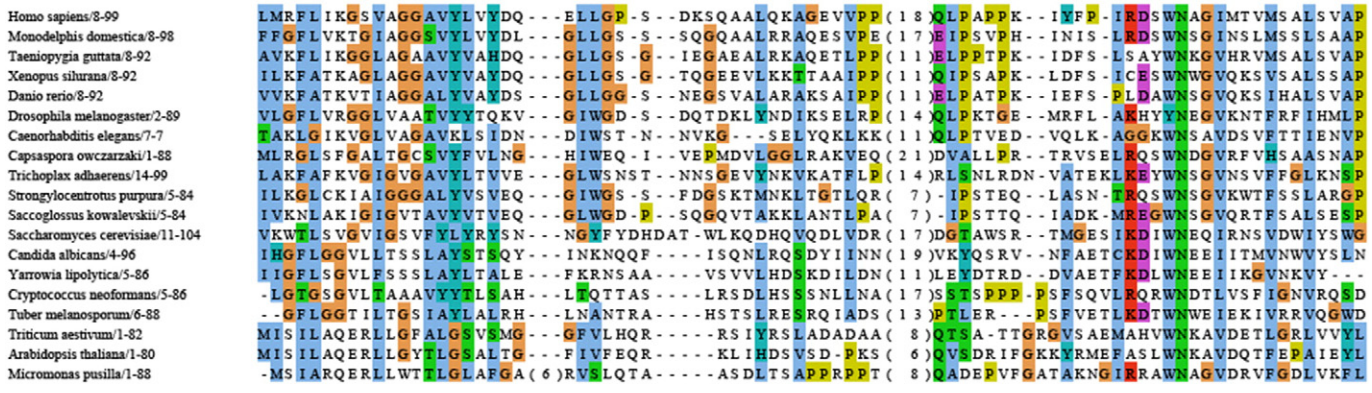

Fig. 2. *Alignment of the Mic12 family among metazoa, fungi and plants + algae* The family shows very little sequence conservation besides an N-terminal hydrophobic region that likely forms a transmembrane helix, and a C-terminal WN motif that tends to be preceded by a positive (K/R) and/or a negatively charged (E/D) amino acid. The W in the WN motif is part of a pattern of conserved hydrophobic residues at distances of 3/4 amino acids, suggesting the presence of an amphipathic helix.

Excavates (*Naegleria*) and therewith substantiating the "potential orthologs" from Munoz-Gomez et al. [20]. Although orthologs of MIC19/MIC25 are widespread among eukaryotes, they have not been detected in the various published mitochondrial proteomes, with the exception of the *C. elegans* CHCH-3 protein [54]. This widespread distribution indicates that, like Mic10, Mic19/25 was present before the radiation of the eukaryotes. Nevertheless, it cannot be detected universally among eukaryotes with cristae. No orthologs could be detected in *Plasmodium*, ciliates or kinetoplasts. As in some of those species other proteins of the Cx9C family have been detected [52], our inability of detecting Mic19/Mic25 orthologs is unlikely to be due to sequence divergence and may reflect the loss of those genes, implying that in those taxa Mic19/Mic25 is not required for the formation of cristae.

3.4. Mic23 and Mic27

Two members represent the Mic23/Mic27 family both in mammals (APOOL/MOMA-1/MIC27 and APOO/MIC23) and in *S. cerevisiae* (Mic26 and Mic27). Based on examination of their phylogeny the two human members of this family have resulted from a duplication at the root of the vertebrates, consistent with their phylogenetic distribution (Fig. 1) while among the fungi in Fig. 1 the protein family is only duplicated in *S. cerevisiae*, resulting from a duplication in the *Saccharomycetales* clade [20]. They are therefore a typical case of many-to-many orthology, and from an evolutionary point of view, as was noted [20], APOO that was recently baptized as MIC26 [55] is not more orthologous to yeast Mic26 than to yeast Mic27, and the name MIC23 appears more appropriate [14]. Do note that this also implies that *S. cerevisiae* Mic27 and mammalian Mic27 are not 1–1 orthologs. Among the metazoa there are in the bony fish (*Danio rerio* in Fig. 1) a few extra duplicated genes in this family, but those are taxon specific, and do not hamper a uniform nomenclature among metazoa. Sensitive homology searches using HHpred do not detect homologs of this family outside the opisthokonts (metazoa and fungi), suggesting that, relative to the other MICOS proteins whose evolutionarily origin can at least be traced back to the root of the eukaryotes, the Mic23/Mic26/Mic27 family is relatively young.

3.5. Mic60

Mic60 (Mitofilin/MINOS2/IMMT/AIM28/FCJ1/FMP13) is widespread among the eukaryotes (Fig. 1). It is e.g. the only MICOS protein for which we can detect homologs in the *Plasmodium*, and is present in mitochondrial protein fractions from fungi [44,56], metazoa [57] and viridiplantae [50](Fig. 1). It is not present in cristae-less species, and, interestingly cannot be detected furthermore in a number of species that do have cristae and Mic10, like the ciliates *Tetrahymena thermophila* and *Paramecium tetraurelia* and the algae *Chlamydomonas*. As has been documented [20], Mic60 has significant sequence similarity to proteins occurring in alphaproteobacteria that contain the mitofilin domain. It therewith appears to be the oldest of the MICOS proteins and, given the alphaproteobacterial ancestry of the mitochondrial membranes and many of its proteins, it seems likely that these proteins were inherited from the alphaproteobacteria.

3.6. A link of bacterial MIC60 homologs to intracellular membranes and to heme synthesis

Alphaproteobacterial MIC60 orthologs, hereafter named MIC60b, occur in species with documented invaginations of the inner membrane, like *Rhodobacter sphaeroides* [58], *Nitrobacter winogradskyi* [59] and *Magnetospirillum magnetoticum* [60]. In *R. sphaeroides* these invaginations become intracytoplasmic membrane bound vesicles [58]. Supporting a direct evolutionary link between these invaginations and cristae, is that the MIC60b of *R. sphaeroides*, RSP_6207, was found to be localized in the membranes of these vesicles, among a total of 52 proteins [61]. Nevertheless, alphaproteobacterial homologs of MIC60 (MIC60b) are not among the "mam–operon" proteins that have been associated with such invaginations in magnetotactic bacteria [60,62]. Genomic context links MIC60b instead to heme synthesis: it tends to have a conserved gene order with the genes for the heme synthesis proteins porphobilinogen deaminase (*HemC*), uroporphyrinogen synthase (*HemD*) and HemY domain containing proteins (Fig. 3A). The link with HemY is particularly strong as MIC60b and the HemY containing proteins are members of orthologous groups (COG4223 and COG3898) that in the STRING database [63] only occur in alphaproteobacteria. Furthermore HemY domain proteins are located in the inner membrane of proteobacteria [64] while MI60b, like MIC60 in eukaryotes, has a single (predicted) transmembrane region [65] (Fig. 3B) and is localized in intracytoplasmic membranes. Interestingly, the *HemC-HemD-HemY* gene cluster also occurs in beta- and gammaproteobacteria. The only difference between the beta/gammaproteobacterial cluster and the alphaproteobacterial cluster is that in the former another gene (*HemX*), appears to have taken the place of *MIC60b* (Fig. 3a). Furthermore, *MIC60b* occurs fused with *HemD* in alphaproteobacteria (e.g. *Rhodospirillum rubrum*) while *HemX* occurs fused with *HemD* in in gammaproteobacteria (e.g. in *Pseudomonas brassicacearum*) and in betaproteobacteria (e.g. in *Neisseria flavescens*). This prompted us to check whether MIC60b is homologous to HemX. Indeed, using profile-profile comparisons [23] we find a distant homology ($E = 0.0044$) of MIC60b proteins with the PFAM domain HemX. The homologous region includes the predicted coiled coil regions, but is not restricted to those and includes the C-terminal mitofilin signature domain. Nevertheless, manual inspection of the alignment between the HemX family and the MIC60b family did not reveal any strongly conserved motifs indicative of a specific interaction (data not shown). The sequence conservation appears rather to reflect an overall alpha-helical structure conservation. The HemX protein in *Escherichia coli* is localized in the inner membrane [66], and, based on its migration profile in a BNE gel likely forms homo-oligomers [66] as has been observed for MIC60 [9]. Just like MIC60 and MIC60b, HemX has an N–terminal transmembrane helix, with the bulk of the protein, including a coiled coil region, predicted to be in the periplasm (Fig. 3b).

There is scant experimental data about the function of HemX in proteobacteria. A fusion gene of *hemX* and *hemD* has been shown to be required for the production of 2-ketogluconate, likely via the heme dependent oxidation of gluconate [67]. Note that HemX from *Bacillus subtilis* [68] and HemX of *Propionibacterium freudenreichii* [69], for which some data do exist, are members of the cytochrome c assembly protein family and the Major Facilitator Superfamily respectively, and are not homologous to HemX from proteobacteria. The intracytoplasmic membrane bound vesicles in *R. sphaeroides* contain the cytochrome $bc_{(1)}$ complex [61], which might explain why MIC60b tends to occur in heme synthesis operons, but not why there is a link between MIC60b and heme synthesis itself. Note that in eukaryotes a MIC60 ortholog occurs in the heme-less species *B. hominis*, while MIC60b does not occur in the heme containing alphaproteobacterium *Rickettsia prowazekii*, so a direct mechanistic involvement of MIC60b in heme synthesis itself appears unlikely.

3.7. SAMM50

The SAMM50 family (SAM50) that has evolved from the bacterial Omp85 family [70]. It is widespread among eukaryotes including the cristae-less species *E. cuniculi* [34], *G. intestinalis*, *E. histolytica* and *T. vaginalis* (Fig. 1) the latter of which actually has the protein in its hydrogenosomal membrane [71]. Moreover it is absent from the genome of the ciliate *Paramecium tetraurelia* (Fig. 1) that does have cristae. It should however be noted that the SAMM50 ortholog in the ciliate *Tetrahymena thermophila* is barely detectable using sequence-profile based searches and was absent from a previous analysis [19]. A

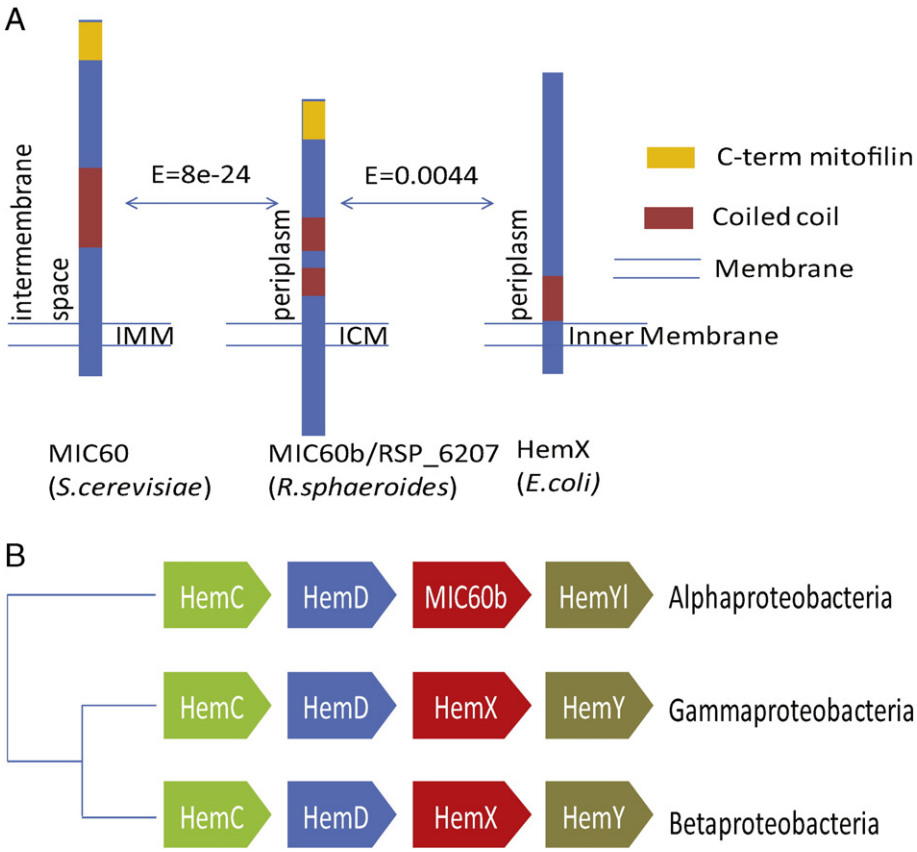

Fig. 3. *Mic60b is associated with heme synthesis in proteobacteria* A) Alphaproteobacterial MIC60 homologs (MIC60b) are part of a conserved gene cluster that appears to be homologous to the *HemC*/*HemD*/*HemX*/*HemY* cluster in beta- and gammaproteobacteria. MIC60b (COG4223) appears to be homologous to HemX (Fig. 3B), while the HemY-like proteins (HemYl, COG3898) are homologous to HemY (COG2959). The MIC60b gene cluster is present among 18 of the alphaproteobacterial genera in STRING (string-db.org). Mainly based on the evolutionary conservation of this operon, the co-occurrence of the *MIC60b* and *HemY-like* genes among genomes, and the fusion of *MIC60b* and *HemD* in a number of species, the likelihood of a functional interaction between MIC60b with HemC, HemD and HemY-like is 0.72, 0.79 and 0.94, respectively [80]. B. *Conservation of the membrane topology of MIC60*, *MIC60b and HemX*. Protein localization in the inner mitochondrial membrane (IMM) [8], IntraCytoplasmic Membranes (ICM) [61] and the inner membrane [66] are based on experimental data from the respective species. The transmembrane topology of MIC60b and HemX was predicted using TMHMM [81]. E-values for homology detection are based on HHpred [23], using an alignment of alphaproteobacterial homologs against an alignment of eukaryotic Mic60 proteins and against the HemX domain from PFAM. "C-term mitofilin" refers to C-terminal mitofilin signature domain using the definition from Zerbes et al. [82]. Coiled coil regions were predicted with coils [83].

SAMM50 homolog in its relative *P. tetrauralia* might thus escape detection using even the most sensitive sequence-based homology detection methods. Despite its interactions with the MICOS complex ([14] and see below), SAMM50 is not known to play a direct role in cristae formation, and its primary function is the assembly of beta-barrel proteins. Indeed, substrates of SAMM50, like TOM40 and the mitochondrial porins have already been observed in species with SAMM50 but without cristae: *E. cuniculi*, *E. histolytica* and *T. vaginalis* [72] while also the cristae-less *G. intestinalis* contains a TOM40 homolog (Fig. 1).

3.8. MTX

The MTX (metaxin) proteins contain a glutathione-S-transferase N-terminal domain and a glutathione-S-transferase C-terminal domain [73] flanked by, among others, a C-terminal transmembrane region. The latter is absent from the most similar proteobacterial homologs that have no signaling peptide either and are likely cytoplasmic. Although these bacterial homologs are the likely ancestors of MTX [74], they probably have a different function and we refrained from calling them orthologs. The phylogenetic relationships between the vertebrate MTX1, MTX2 and MTX3, their homolog "failed axon connections" (FAXC) [75], and the members of this family in *S. pombe* (Mtx1, Mtxl) and *S. cerevisiae* (Sam35, Sam37) cannot confidently be resolved, neither from sequence similarity levels nor from phylogenies due to lack of sequence similarity of Sam35 with MTX in other eukaryotes (data not shown). We tentatively have grouped them in Fig. 1, but we cannot exclude that Sam35 and Sam37 result from a gene duplication that is independent from the one that lead to MTX1 and MTX2. MTX1 and MTX3 have resulted from gene duplication at the root of the vertebrates (Fig. 1) [25]. MTX proteins only occur in species with cristae, but are not universal among them (Fig. 1), and they rather appear to occur in a subset of genomes with SAMM50.

3.9. DNAJC11

DNAJC11 has been implicated to form a complex with SAMM50 [13], has been shown to interact with components of the MICOS complex [11] and seems to be required for proper cristae formation [76]. The protein contains, aside from an N-terminal DNAJ domain, also a well-conserved C-terminal domain DUF3395 [76]. Although this domain occurs in some bacterial proteins, in those proteins it does not occur in conjunction with the DNAJ domain. Furthermore we did not detect homologs in alphaproteobacteria, and the bacterial DUF3395 homologs may have been the result of horizontal gene transfer from eukaryotes to bacteria. Orthologs of DNACJ11 are readily identifiable throughout the eukaryotes, indicating their origin at the root of the eukaryotes, and occur only in species with cristae (Fig. 1). However, a few species with cristae, including *S. cerevisiae*, do not have a DNAJC11 ortholog.

3.10. Complexome profiling of MICOS and MIB components

Blue-native electrophoresis (BNE) of mitochondria reveals large complexes of different size that contain different components of the MIB complexes [14]. To study the distribution and composition of these complexes in detail, we analyzed digitonin-solubilized mitochondria from human cell lines by complexome profiling [21]. This method allows the assignment of proteins identified by mass spectrometry to different complexes based on similarities in their migration profiles in the BNE gels. Their relative distribution can be estimated by label-free quantification. A representative complexome profiling analysis of the MICOS and MIB complexes in mitochondria from human 143B cells performed by bottom-up hierarchical clustering in combination with correlation profiling of additional candidate proteins is shown in Fig. 4. Panel A shows a heatmap representation of the migration profiles of the identified components (Table 1). No other proteins in the complete complexome profiles of mitochondria from 143B osteosarcoma cells exhibited a migration pattern that would have allowed assigning them to the complexes under study here.

Table 1
Proteomics data of identified MIB components[a].

Protein	*M_r*	*Peptides identified*		*Sequence coverage*
	kDa	Total	Unique	%
MIC10	7.0	2	2	24
MIC12	13.1	5	5	74
MIC19	26.2	12	12	39
MIC25	26.5	7	7	43
MIC23	22.3	5	5	34
MIC27	29.2	15	15	69
MIC60	82.6	47	2[b]	66
SAMM50	52.0	25	25	59
MTX2	29.8	10	10	58
MTX3	28.6	7	2	32
MTX1	51.5	11	11	51
DNAJC11	63.3	21	21	48

[a] Values from a combined analysis of three replicates of representative complexome profile of mitochondria from 143B cells.
[b] All three isoforms of MIC60 were found based on 1–2 variant specific isoforms. Since no isoform specific migration profile could be identified, the abundance values of the three isoforms were averaged. In this the parameters for isoform 3 are given and the low number of unique peptides reflects the overlap with the other isoforms.

3.11. The MICOS complex

With the recently discovered QIL1/C19orf70 [11] shown here to be the mammalian ortholog of Mic12 (Fig. 2), all seven constituents of the MICOS complex showed very similar migration patterns with a pronounced maximum at around 700 kDa. However, in all profiles analyzed, MIC60, MIC19 and MIC25 consistently occurred in significant amounts already at about 450 kDa and above, confirming previous observations [11,77]. In contrast, the remaining MICOS components showed a steep increase in abundance only from and above 600 kDa. This suggested that these three proteins form a centerpiece around which the remaining proteins arrange to form the full size MICOS complex.

3.12. The MIB complex

Of the outer membrane components of the MIB complex, SAMM50, MTX1, MTX2 and DNAJC11 co-migrated together only at about

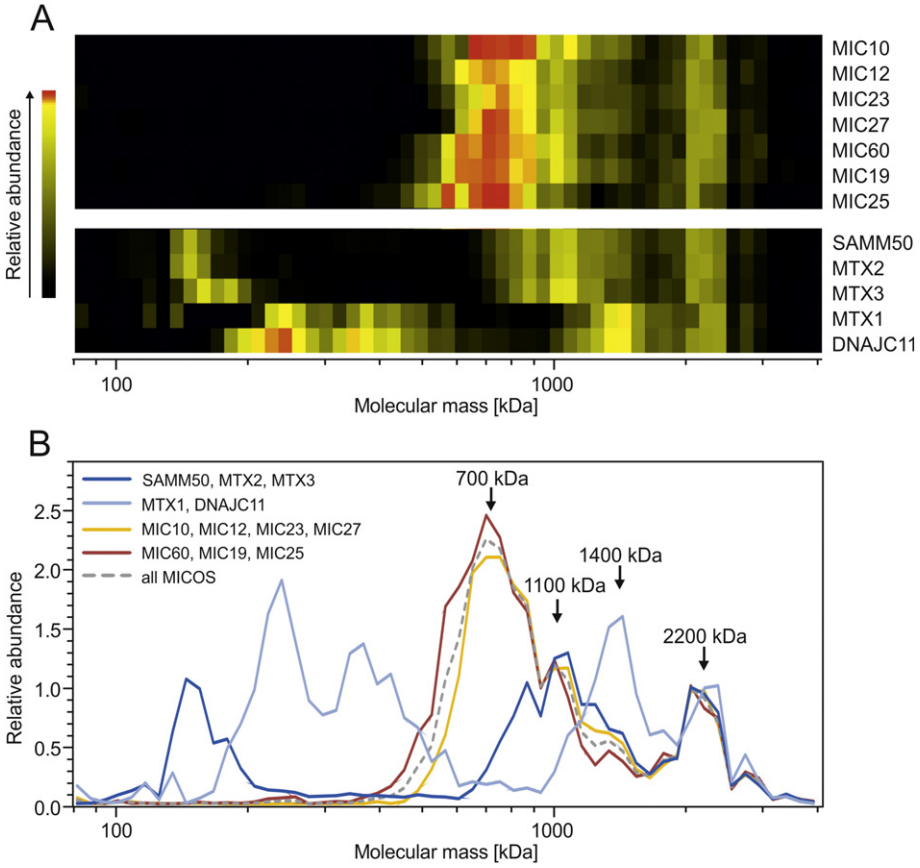

Fig. 4. *Complexome profiling analysis of the MICOS and MIB complexes in human 143B cells.* Migration patterns of MIB proteins were extracted from a complexome profile of digitonin solubilized mitochondria prepared from human 143B cells. A dataset representative for experiments with five independent batches of mitochondria is shown. Profiles from three technical replicates obtained with the same mitochondrial preparation and run in the same gel were averaged and abundance values were normalized setting the intensity at 2200 kDa to unity. A, heatmap representation of individual migration profiles; B, averaged abundance profiles of subassemblies as indicated in the legend. MICOS (dashed line) represents the average profile of all seven MICOS components. See text for further details.

2200 kDa, where also all components of the MICOS complex showed a clear peak in abundance. In addition, we found that MTX3 exhibited a migration profile that was very similar to that of MTX2. This identifies this protein of previously unknown function as another component of the MIB complex. At lower masses, two clearly distinct migration patterns of the outer membrane components divided them into two groups. SAMM50, MTX2 and MTX3 showed a peak of abundance at around 1100 kDa and were present in complexes in the range below 200 kDa as well. In contrast, MTX1 and DNAJC11 showed a clear maximum at about 1400 kDa and occurred in multiple smaller complexes in the range between 200 and 500 kDa. The co-migration pattern in the mass range up to 500 kDa suggested that SAMM50/MTX2/MTX3 and MTX1/DNAJ11 formed subassemblies that both appear to be part of the MIB complex.

3.13. Subassemblies of the MIB complex

To define the observed complexes more clearly, we averaged the relative amounts of the components of the subassemblies and plotted their relative abundance against the molecular mass (Fig. 4B). For a quantitative estimate of the relative distribution of the subcomplexes, we normalized the profiles, setting the abundance at 2200 kDa to unity. For the MICOS complex, a clear separation between the average of MIC60, MIC19 and MIC25 and that of the four remaining proteins further supports the notion of a centerpiece version of this complex around MIC60 as the largest and most ancient constituent of the complex. Although it was not possible to determine the absolute number of the components, the similar relative abundance of all MICOS proteins suggested that the stoichiometry of its components remained essentially the same when it associated with other proteins to form the larger complexes. The profile of SAMM50/MTX2/MTX3 seems to indicate that together these components progressively add to the MICOS complex to form small versions of the MIB complex of about 800 kDa, 1100 kDa and 1400 kDa. Addition of MTX1/DNAJC11 then gives the full size 2200 kDa MIB complex, possibly by recruitment of two or three copies of the ~350 kDa subassembly of these proteins by the 1100 kDa and 1400 kDa MIB subcomplexes. The large peak of the MTX1/DNAJC11 subassembly at 1400 kDa could then be a tetramer of the 350 kDa complex that could associate with the 1400 kDa subcomplex explaining the largest version of the MIB complex observed in small amounts at 2800 kDa (Fig. 6). The mismatch in abundance renders it unlikely that the MTX1/DNAJC11 subassembly is a component of the 1400 kDa MIB subcomplex.

3.14. MICOS and MIB complexes in human skin fibroblasts

To corroborate our observations from 143B cells, we also analyzed the MICOS and MIB complexes in complexome profiles of mitochondria from human skin fibroblast cell lines that proliferate much more slowly than the tumor cell line used for the initial characterization. We observed the same complexes and subassemblies as in the profiles of mitochondria from 143B cells (Fig. 4), but their relative distribution was distinctly different. Fig. 5 shows a characteristic profile of the MICOS and MIB components seen in several datasets, in which the largest version of the MIB complex was the dominant species, while the 700 kDa MICOS complex that was most prominent in mitochondria from 143B cells was not detectable at all. In other complexome profiles of fibroblast mitochondria this shift to larger assemblies was less extreme and significant amounts of the 700 kDa MICOS complex were still present (not shown).

4. Discussion

Of the main MIB subcomplexes we find a strong correlation of MICOS proteins and of DNAJC11 with the documented occurrence of cristae: species without cristae never have MICOS proteins or DNAJC11, and all species with cristae have at least one MICOS protein and almost all have DNAJC11. With respect to the MICOS proteins this is consistent with the observations of Munoz-Gomez et al. [20], while we can substantiate their "putative orthologs" of MIC19/25 outside the fungi and the metazoa. Nevertheless our observations with respect to Mic12 indicate for a more widespread phylogenetic distribution than was established and show that it can be traced back to the root of the eukaryotes. Mic10 is the most widespread protein of the MICOS proteins, being the only MICOS protein that can e.g. be found in ciliates and in kinetoplasts. Not all MICOS proteins can however be found in all species with cristae. This can be explained in part by the evolutionary late origin of the Mic23/Mic26/Mic27 family that is only present in the opisthokonts. Moreover, homology detection by sequence comparison reaches its limits in the short and rapidly evolving Mic12 family originally described in fungi, as it is barely detectable in metazoa and plants. Nevertheless, such explanations do not apply to Mic60, a large and relatively well-conserved protein predating mitochondria, which has been lost multiple times during evolution in cristae containing species, while Mic10, the other "core" protein of the MICOS complex, has been conserved. Our complexome profiling data suggested that MIC60 is part of a MICOS centerpiece also observed in mitochondria from a MIC12 knockdown cell line [11]. The presence of cristae in species lacking Mic60, but containing Mic10 may then suggest that the MIC60 containing MICOS subcomplex is a non-essential scaffold that could be involved in recruiting MIC10 and other proteins and may stabilize the MIB complex.

The origin of Mic60 in alphaproteobacteria strengthens the link between mitochondria and alphaproteobacteria [20]. That a member of this protein family is found in intracytoplasmic membranes in the alphaproteobacterium *R. sphaeroides* provides initial evidence that these membrane structures are directly related to cristae. Interestingly, we find that this protein family is likely even older, and can be traced back to the root of the alpha-, beta- and gammaproteobacteria where it is has a strong link to heme synthesis via a conserved gene cluster in their genomes. Experimental characterization of the function of MIC60b and of HemX might provide a clue to the common evolutionary origin of cristae in mitochondria and of intracytoplasmic membranes in alphaproteobacteria.

By significant similarity at the sequence profile level, we provide evidence that QIL1/C19orf70 is the ortholog of Mic12 from yeast. QIL1/C19orf70 was most recently assigned and characterized as a novel protein of the MICOS complex by Guarani et al. [11] and we found it to comigrate with the other MICOS proteins, which is consistent with a conserved function in MICOS. In *S. cerevisiae*, the deletion of Mic12 results in only a partial dissociation of the MICOS complex [78]. In a human cell line, Guarani et al. also observed dissociation of the MICOS complex after MIC12 deletion with a decrease in MIC10, MIC26 and MIC27 [11]. This argues for a more essential role of MIC12 in mammalian cells than in yeast, where its absence does not have any effect on the steady state levels of other MICOS components and does not result in a severe morphology defect [78,79].

Overall, both the evolutionary analysis and the complexome profiling data further establish MICOS as a rather robustly defined complex of the inner mitochondrial membrane centrally involved in cristae formation. Although MIC60, MIC19 and MIC25 seem to form a centerpiece of this structure that can exist without the other MICOS proteins that also accumulates after MIC12 knockdown in human cells [11], the absence of Mic60 in some cristae forming species suggests that this subassembly is functionally not essential.

For the outer membrane components of the MIB complex, we could define two subassemblies assigning distinct roles to MTX1 and MTX2. We also identified MTX3, a vertebrate specific paralog of MTX1, as a probably new component of the MIB complex. Remarkably, the SAMM50/MTX2/MTX3 subassembly is sufficient to recruit the MICOS complex to form the MIB centerpiece structure. As possible stabilizing factors, MTX1 together with DNAJC11, a protein not found in yeast, add on to give the full size human MIB complex.

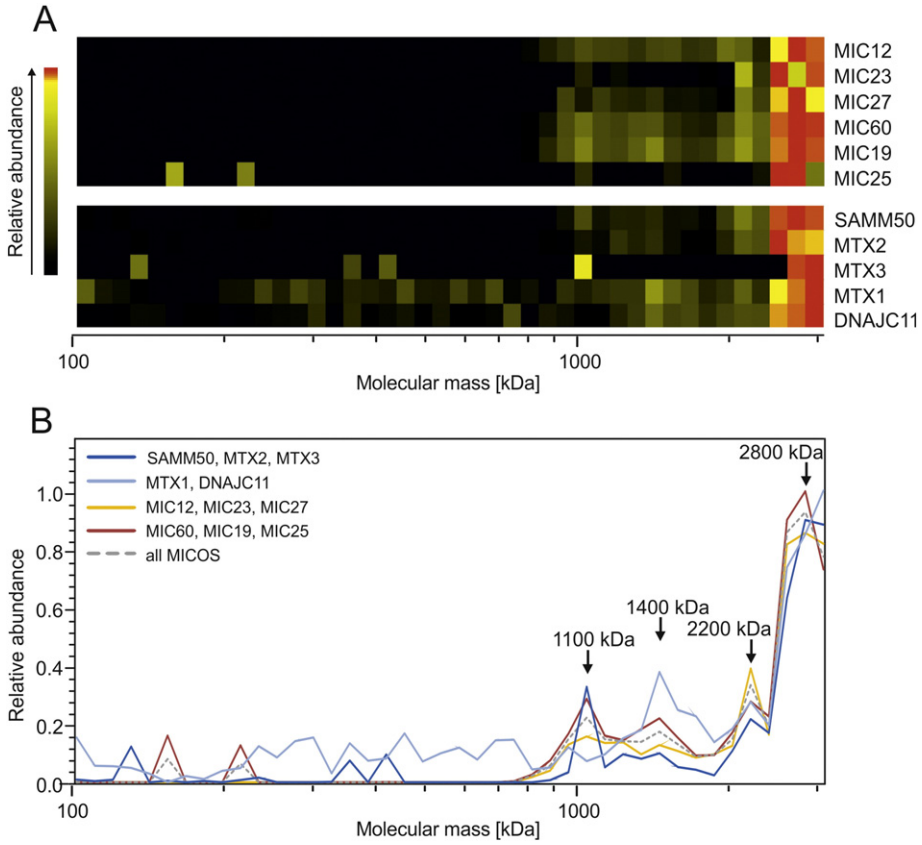

Fig. 5. *Complexome profiling analysis of the MICOS and MIB complexes in human skin fibroblasts.* Migration patterns of MIB proteins were extracted from a complexome profile of digitonin solubilized mitochondria prepared from human skin fibroblast (cell line C-5120 from the Nijmegen Center for Mitochondrial Disorders). A characteristic dataset is shown. MIC10 was not detected in this particular dataset, but was found associated with MICOS and MIB in other complexome profiles from fibroblast mitochondria (data not shown). Abundance values were normalized, setting the intensity at 2800 kDa to unity. A, heatmap representation of individual migration profiles; B, abundance profiles of subassemblies as indicated in the legend. MICOS (dashed line) represents the average profile of all seven MICOS components. See text for further details.

In summary, complexome profiling of mitochondria provided evidence for defined subassemblies leading from a MICOS centerpiece complex to the full size 2200/2800 kDa MIB complex (Fig. 6) that seem to correlate with the complexes of different size and abundance observed by Ott et al. [14]. Although we cannot exclude at this point that some of the observed subcomplexes were degradation products, or resulted from partial dissociation of the components during electrophoresis, they do provide useful insights into the architecture of the MIB complex. It is tempting to speculate that the observed complexes may reflect a set of intermediates present in the mitochondrial membranes, which dynamically interact in a stepwise assembly pathway to eventually form the large structure bridging the inner and outer mitochondrial membrane that is needed for cristae formation. Interestingly, the 2800 kDa full size MIB complex was much more prominent in mitochondria from human skin fibroblasts than in those from the tumor cell line. This is consistent with increase stability and reduced dynamics of cristae in these differentiated and more slowly proliferating fibroblasts.

Conflict of interest

The authors declare that they have no conflict of interest.

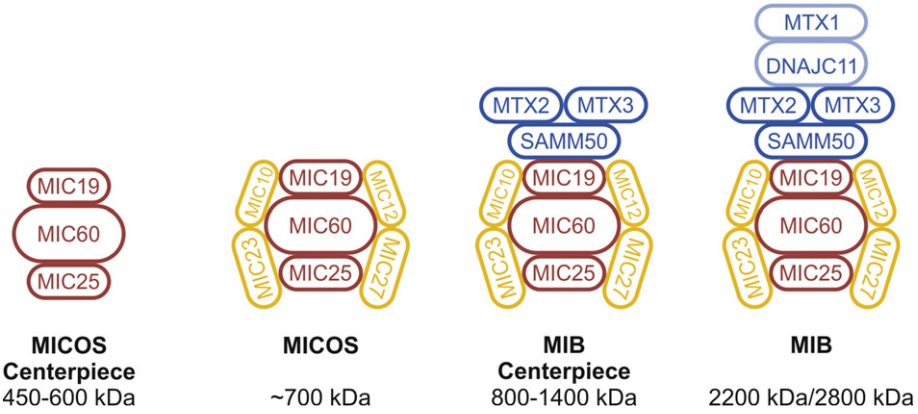

Fig. 6. *Schematic representation of MICOS and MIB complex intermediates as defined by complexome profiling.* Note that most proteins and subassemblies are probably present as multiple copies, and the scheme does not include information on the stoichiometries. See text for further details.

Acknowledgments

We wish to thank the referees for their constructive comments. This work was supported by a grant of the Excellence Initiative of the German Federal and State Governments (EXC115) to U.B. and a Fellowship of the Humboldt Foundation to S.G. MAH is supported by the Virgo Consortium, funded by the Dutch government (FES0908), and by The Netherlands Genomics Initiative (050-060-452).

Appendix A. Supplementary data

Supplementary data to this article can be found online at http://dx.doi.org/10.1016/j.bbamcr.2015.10.009.

References

[1] G.E. Palade, An electron microscope study of the mitochondrial structure, J. Histochem. Cytochem. 1 (1953) 188–211.
[2] G.E. Palade, The fine structure of mitochondria, Anat. Rec. 114 (1952) 427–451.
[3] M.A. Rudzinska, A.W. Sedar, Mitochondria of protozoa, J. Biophys. Biochem. Cytol. 2 (1956) 331–336.
[4] H.A. Lund, A.E. Vatter, J.B. Hanson, Biochemical and cytological changes accompanying growth and differentiation in the roots of Zea mays, J. Biophys. Biochem. Cytol. 4 (1958) 87–98.
[5] B. Boxma, R.M. de Graaf, G.W. van der Staay, et al., An anaerobic mitochondrion that produces hydrogen, Nature 434 (2005) 74–79.
[6] R.M. Zerbes, I.J. van der Klei, M. Veenhuis, N. Pfanner, M. van der Laan, M. Bohnert, Mitofilin complexes: conserved organizers of mitochondrial membrane architecture, Biol. Chem. 393 (2012) 1247–1261.
[7] N. Pfanner, M. van der Laan, P. Amati, et al., Uniform nomenclature for the mitochondrial contact site and cristae organizing system, J. Cell Biol. 204 (2014) 1083–1086.
[8] G.B. John, Y. Shang, L. Li, C. Renken, C.A. Mannella, J.M. Selker, L. Rangell, M.J. Bennett, J. Zha, The mitochondrial inner membrane protein mitofilin controls cristae morphology, Mol. Biol. Cell 16 (2005) 1543–1554.
[9] R. Rabl, V. Soubannier, R. Scholz, et al., Formation of cristae and crista junctions in mitochondria depends on antagonism between Fcj1 and Su e/g, J. Cell Biol. 185 (2009) 1047–1063.
[10] J.Y. Mun, T.H. Lee, J.H. Kim, B.H. Yoo, Y.Y. Bahk, H.S. Koo, S.S. Han, Caenorhabditis elegans mitofilin homologs control the morphology of mitochondrial cristae and influence reproduction and physiology, J. Cell. Physiol. 224 (2010) 748–756.
[11] V. Guarani, E.M. McNeill, J.A. Paulo, E.L. Huttlin, F. Frohlich, S.P. Gygi, D. Van Vactor, J.W. Harper, QIL1 is a novel mitochondrial protein required for MICOS complex stability and cristae morphology, Elife 4 (2015).
[12] N. Pfanner, N. Wiedemann, C. Meisinger, T. Lithgow, Assembling the mitochondrial outer membrane, Nat. Struct. Mol. Biol. 11 (2004) 1044–1048.
[13] J. Xie, M.F. Marusich, P. Souda, J. Whitelegge, R.A. Capaldi, The mitochondrial inner membrane protein mitofilin exists as a complex with SAM50, metaxins 1 and 2, coiled-coil-helix coiled-coil-helix domain-containing protein 3 and 6 and DnaJC11, FEBS Lett. 581 (2007) 3545–3549.
[14] C. Ott, E. Dorsch, M. Fraunholz, S. Straub, V. Kozjak-Pavlovic, Detailed analysis of the human mitochondrial contact site complex indicate a hierarchy of subunits, PLoS One 10 (2015), e0120213.
[15] R. Szklarczyk, B.F. Wanschers, T.D. Cuypers, et al., Iterative orthology prediction uncovers new mitochondrial proteins and identifies C12orf62 as the human ortholog of COX14, a protein involved in the assembly of cytochrome c oxidase, Genome Biol. 13 (2012) R12.
[16] T. Gabaldon, D. Rainey, M.A. Huynen, Tracing the evolution of a large protein complex in the eukaryotes, NADH:ubiquinone oxidoreductase (complex I), J. Mol. Biol. 348 (2005) 857–870.
[17] I. Ogilvie, N.G. Kennaway, E.A. Shoubridge, A molecular chaperone for mitochondrial complex I assembly is mutated in a progressive encephalopathy, J. Clin. Invest. 115 (2005) 2784–2792.
[18] L. Delage, C. Leblanc, P. Nyvall Collen, B. Gschloessl, M.P. Oudot, L. Sterck, J. Poulain, J.M. Aury, J.M. Cock, In silico survey of the mitochondrial protein uptake and maturation systems in the brown alga ectocarpus siliculosus, PLoS One 6 (2011), e19540.
[19] M. Wojtkowska, M. Jakalski, J.R. Pienkowska, O. Stobienia, A. Karachitos, T.M. Przytycka, J. Weiner 3rd, H. Kmita, W. Makalowski, Phylogenetic analysis of mitochondrial outer membrane beta-barrel channels, Genome Biol. Evol. 4 (2012) 110–125.
[20] S.A. Munoz-Gomez, C.H. Slamovits, J.B. Dacks, K.A. Baier, K.D. Spencer, J.G. Wideman, Ancient homology of the mitochondrial contact site and cristae organizing system points to an endosymbiotic origin of mitochondrial cristae, Curr. Biol. 25 (2015) 1489–1495.
[21] H. Heide, L. Bleier, M. Steger, et al., Complexome profiling identifies TMEM126B as a component of the mitochondrial complex I assembly complex, Cell Metab. 16 (2012) 538–549.
[22] R.D. Finn, J. Clements, W. Arndt, B.L. Miller, T.J. Wheeler, F. Schreiber, A. Bateman, S.R. Eddy, HMMER web Server: 2015 Update, Nucleic Acids Res. (2015).
[23] J. Soding, Protein homology detection by HMM-HMM comparison, Bioinformatics 21 (2005) 951–960.
[24] R.D. Finn, A. Bateman, J. Clements, et al., Pfam: the protein families database, Nucleic Acids Res. 42 (2014) D222–D230.
[25] F. Schreiber, M. Patricio, M. Muffato, M. Pignatelli, A. Bateman, TreeFam v9: a new website, more species and orthology-on-the-fly, Nucleic Acids Res. 42 (2014) D922–D925.
[26] A.C. Smith, J.A. Blackshaw, A.J. Robinson, MitoMiner: a data warehouse for mitochondrial proteomics data, Nucleic Acids Res. 40 (2012) D1160–D1167.
[27] I. Wittig, H.P. Braun, H. Schagger, Blue native PAGE, Nat. Protoc. 1 (2006) 418–428.
[28] M.O. Collins, L. Yu, I. Campuzano, S.G. Grant, J.S. Choudhary, Phosphoproteomic analysis of the mouse brain cytosol reveals a predominance of protein phosphorylation in regions of intrinsic sequence disorder, Mol. Cell. Proteomics 7 (2008) 1331–1348.
[29] H.J. Wessels, R.O. Vogel, R.N. Lightowlers, et al., Analysis of 953 human proteins from a mitochondrial HEK293 fraction by complexome profiling, PLoS One 8 (2013), e68340.
[30] J.V. Olsen, L.M. de Godoy, G. Li, et al., Parts per million mass accuracy on an orbitrap mass spectrometer via lock mass injection into a C-trap, Mol. Cell. Proteomics 4 (2005) 2010–2021.
[31] J. Cox, M. Mann, MaxQuant enables high peptide identification rates, individualized p.p.b.-range mass accuracies and proteome-wide protein quantification, Nat. Biotechnol. 26 (2008) 1367–1372.
[32] H. Giese, J. Ackermann, H. Heide, L. Bleier, S. Drose, I. Wittig, U. Brandt, I. Koch, NOVA: a software to analyze complexome profiling data, Bioinformatics 31 (2015) 440–441.
[33] S. Sharma, U.K. Singha, M. Chaudhuri, Role of Tob55 on mitochondrial protein biogenesis in trypanosoma brucei, Mol. Biochem. Parasitol. 174 (2010) 89–100.
[34] P. Dolezal, M.J. Dagley, M. Kono, et al., The essentials of protein import in the degenerate mitochondrion of entamoeba histolytica, PLoS Pathog. 6 (2010), e1000812.
[35] A.D. Tsaousis, E.R. Kunji, A.V. Goldberg, J.M. Lucocq, R.P. Hirt, T.M. Embley, A novel route for ATP acquisition by the remnant mitochondria of encephalitozoon cuniculi, Nature 453 (2008) 553–556.
[36] S. Ghosh, J. Field, R. Rogers, M. Hickman, J. Samuelson, The entamoeba histolytica mitochondrion-derived organelle (crypton) contains double-stranded DNA and appears to be bound by a double membrane, Infect. Immun. 68 (2000) 4319–4322.
[37] J. Tovar, G. Leon-Avila, L.B. Sanchez, R. Sutak, J. Tachezy, M. van der Giezen, M. Hernandez, M. Muller, J.M. Lucocq, Mitochondrial remnant organelles of giardia function in iron-sulphur protein maturation, Nature 426 (2003) 172–176.
[38] M. Muller, Biochemical cytology of trichomonad flagellates. I. Subcellular localization of hydrolases, dehydrogenases, and catalase in tritrichomonas foetus, J. Cell Biol. 57 (1973) 453–474.
[39] A.K. Alkhaja, D.C. Jans, M. Nikolov, et al., MINOS1 is a conserved component of mitofilin complexes and required for mitochondrial function and cristae organization, Mol. Biol. Cell 23 (2012) 247–257.
[40] M. Bohnert, R.M. Zerbes, K.M. Davies, et al., Central role of Mic10 in the mitochondrial contact site and cristae organizing system, Cell Metab. 21 (2015) 747–755.
[41] M. Barbot, D.C. Jans, C. Schulz, N. Denkert, B. Kroppen, M. Hoppert, S. Jakobs, M. Meinecke, Mic10 oligomerizes to bend mitochondrial inner membranes at cristae junctions, Cell Metab. 21 (2015) 756–763.
[42] W.P. Russ, D.M. Engelman, The GxxxG motif: a framework for transmembrane helix-helix association, J. Mol. Biol. 296 (2000) 911–919.
[43] J.L. Heazlewood, J.S. Tonti-Filippini, A.M. Gout, D.A. Day, J. Whelan, A.H. Millar, Experimental analysis of the arabidopsis mitochondrial proteome highlights signaling and regulatory components, provides assessment of targeting prediction programs, and indicates plant-specific mitochondrial proteins, Plant Cell 16 (2004) 241–256.
[44] A. Matsuyama, R. Arai, Y. Yashiroda, et al., ORFeome cloning and global analysis of protein localization in the fission yeast Schizosaccharomyces pombe, Nat. Biotechnol. 24 (2006) 841–847.
[45] C.H. Zierdt, H.K. Tan, Ultrastructure and light microscope appearance of blastocystis hominis in a patient with enteric disease, Z. Parasitenkd. 50 (1976) 277–283.
[46] F. Denoeud, M. Roussel, B. Noel, et al., Genome sequence of the stramenopile blastocystis, a human anaerobic parasite, Genome Biol. 12 (2011), R29.
[47] J.S. Keithly, S.G. Langreth, K.F. Buttle, C.A. Mannella, Electron tomographic and ultrastructural analysis of the cryptosporidium parvum relict mitochondrion, its associated membranes, and organelles, J. Eukaryot. Microbiol. 52 (2005) 132–140.
[48] M. Uhlen, L. Fagerberg, B.M. Hallstrom, et al., Proteomics. Tissue-based map of the human proteome, Science 347 (2015) (1260419).
[49] N. Lefort, Z. Yi, B. Bowen, et al., Proteome profile of functional mitochondria from human skeletal muscle using one-dimensional gel electrophoresis and HPLC-ESI-MS/MS, J. Proteome 72 (2009) 1046–1060.
[50] J. Klodmann, M. Senkler, C. Rode, H.P. Braun, Defining the protein complex proteome of plant mitochondria, Plant Physiol. 157 (2011) 587–598.
[51] K. Peters, K. Belt, H.P. Braun, 3D gel map of arabidopsis complex I, Front. Plant Sci. 4 (2013) 153.
[52] G. Cavallaro, Genome-wide analysis of eukaryotic twin CX9C proteins, Mol. BioSyst. 6 (2010) 2459–2470.
[53] R. Szklarczyk, M.A. Huynen, Expansion of the human mitochondrial proteome by intra- and inter-compartmental protein duplication, Genome Biol. 10 (2009), R135.
[54] B.P. Head, M. Zulaika, S. Ryazantsev, A.M. van der Bliek, A novel mitochondrial outer membrane protein, MOMA-1, that affects cristae morphology in Caenorhabditis elegans, Mol. Biol. Cell 22 (2011) 831–841.
[55] S. Koob, M. Barrera, R. Anand, A.S. Reichert, The non-Glycosylated Isoform of MIC26 is a Constituent of the Mammalian MICOS Complex and Promotes Formation of Crista Junctions, Biochim. Biophys. Acta 1853 (7) (2015) 1551–1563.
[56] S. Schmitt, H. Prokisch, T. Schlunck, et al., Proteome analysis of mitochondrial outer membrane from Neurospora crassa, Proteomics 6 (2006) 72–80.

[57] S. Yin, J. Xue, H. Sun, et al., Quantitative evaluation of the mitochondrial proteomes of Drosophila melanogaster adapted to extreme oxygen conditions, PLoS One 8 (2013), e74011.
[58] J.D. Tucker, C.A. Siebert, M. Escalante, P.G. Adams, J.D. Olsen, C. Otto, D.L. Stokes, C.N. Hunter, Membrane invagination in rhodobacter sphaeroides is initiated at curved regions of the cytoplasmic membrane, then forms both budded and fully detached spherical vesicles, Mol. Microbiol. 76 (2010) 833–847.
[59] E. Bock, G. Heinrich, Structural and functional changes in reactivating cells of nitrobacter winogradskyi buch, Arch. Mikrobiol. 77 (1971) 349–365.
[60] H. Nudelman, R. Zarivach, Structure prediction of magnetosome-associated proteins, Front. Microbiol. 5 (2014) 9.
[61] G.M. D'Amici, S. Rinalducci, L. Murgiano, F. Italiano, L. Zolla, Oligomeric characterization of the photosynthetic apparatus of rhodobacter sphaeroides R26.1 by nondenaturing electrophoresis methods, J. Proteome Res. 9 (2010) 192–203.
[62] M. Richter, M. Kube, D.A. Bazylinski, T. Lombardot, F.O. Glockner, R. Reinhardt, D. Schuler, Comparative genome analysis of four magnetotactic bacteria reveals a complex set of group-specific genes implicated in magnetosome biomineralization and function, J. Bacteriol. 189 (2007) 4899–4910.
[63] C. von Mering, M. Huynen, D. Jaeggi, S. Schmidt, P. Bork, B. Snel, STRING: a database of predicted functional associations between proteins, Nucleic Acids Res. 31 (2003) 258–261.
[64] D.O. Daley, M. Rapp, E. Granseth, K. Melen, D. Drew, G. von Heijne, Global topology analysis of the Escherichia coli inner membrane proteome, Science 308 (2005) 1321–1323.
[65] E.L. Sonnhammer, G. von Heijne, A. Krogh, A hidden markov model for predicting transmembrane helices in protein sequences, Proc. Int. Conf. Intell. Syst. Mol. Biol. 6 (1998) 175–182.
[66] F. Stenberg, P. Chovanec, S.L. Maslen, C.V. Robinson, L.L. Ilag, G. von Heijne, D.O. Daley, Protein complexes of the Escherichia coli cell envelope, J. Biol. Chem. 280 (2005) 34409–34419.
[67] P.L. Hsu, L. Condron, M. O'Callaghan, M.R. Hurst, hemX is required for production of 2-ketogluconate, the predominant organic anion required for inorganic phosphate solubilization by Burkholderia sp. Ha185, Environ. Microbiol. Rep. (2015).
[68] I. Schroder, P. Johansson, L. Rutberg, L. Hederstedt, The hemX gene of the Bacillus subtilis hemAXCDBL operon encodes a membrane protein, negatively affecting the steady-state cellular concentration of HemA (glutamyl-tRNA reductase), Microbiology 140 (Pt 4) (1994) 731–740.
[69] Y. Hashimoto, M. Yamashita, Y. Murooka, The propionibacterium freudenreichii hemYHBXRL gene cluster, which encodes enzymes and a regulator involved in the biosynthetic pathway from glutamate to protoheme, Appl. Microbiol. Biotechnol. 47 (1997) 385–392.
[70] I. Gentle, K. Gabriel, P. Beech, R. Waller, T. Lithgow, The Omp85 family of proteins is essential for outer membrane biogenesis in mitochondria and bacteria, J. Cell Biol. 164 (2004) 19–24.
[71] C.J. Kay, K. Lawler, I.D. Kerr, Analysis of the Sam50 translocase of excavate organisms supports evolution of divergent organelles from a common endosymbiotic event, Biosci. Rep. 33 (2013).
[72] D.C. Bay, M. Hafez, M.J. Young, D.A. Court, Phylogenetic and coevolutionary analysis of the beta-barrel protein family comprised of mitochondrial porin (VDAC) and Tom40, Biochim. Biophys. Acta 1818 (2012) 1502–1519.
[73] K.W. Adolph, Characterization of the cDNA and amino acid sequences of xenopus metaxin 3, and relationship to xenopus metaxins 1 and 2, DNA Seq. 16 (2005) 252–259.
[74] S. Kutik, D.A. Stroud, N. Wiedemann, N. Pfanner, Evolution of mitochondrial protein biogenesis, Biochim. Biophys. Acta 1790 (2009) 409–415.
[75] K.K. Hill, V. Bedian, J.L. Juang, F.M. Hoffmann, Genetic interactions between the drosophila abelson (Abl) tyrosine kinase and failed axon connections (fax), a novel protein in axon bundles, Genetics 141 (1995) 595–606.
[76] F. Ioakeimidis, C. Ott, V. Kozjak-Pavlovic, et al., A splicing mutation in the novel mitochondrial protein DNAJC11 causes motor neuron pathology associated with cristae disorganization, and lymphoid abnormalities in mice, PLoS One 9 (2014), e104237.
[77] M. Darshi, V.L. Mendiola, M.R. Mackey, A.N. Murphy, A. Koller, G.A. Perkins, M.H. Ellisman, S.S. Taylor, ChChd3, an inner mitochondrial membrane protein, is essential for maintaining crista integrity and mitochondrial function, J.Biol. Chem. 286 (2011) 2918–2932.
[78] S. Hoppins, S.R. Collins, A. Cassidy-Stone, et al., A mitochondrial-focused genetic interaction map reveals a scaffold-like complex required for inner membrane organization in mitochondria, J. Cell Biol. 195 (2011) 323–340.
[79] K. von der Malsburg, J.M. Muller, M. Bohnert, et al., Dual role of mitofilin in mitochondrial membrane organization and protein biogenesis, Dev. Cell 21 (2011) 694–707.
[80] B. Snel, G. Lehmann, P. Bork, M.A. Huynen, STRING: a web-server to retrieve and display the repeatedly occurring neighbourhood of a gene, Nucleic Acids Res. 28 (2000) 3442–3444.
[81] A. Krogh, B. Larsson, G. von Heijne, E.L. Sonnhammer, Predicting transmembrane protein topology with a hidden markov model: application to complete genomes, J. Mol. Biol. 305 (2001) 567–580.
[82] R.M. Zerbes, M. Bohnert, D.A. Stroud, et al., Role of MINOS in mitochondrial membrane architecture: cristae morphology and outer membrane interactions differentially depend on mitofilin domains, J. Mol. Biol. 422 (2012) 183–191.
[83] A. Lupas, M. Van Dyke, J. Stock, Predicting coiled coils from protein sequences, Science 252 (1991) 1162–1164.